ANALYSIS AND DESIGN OF AXIALLY LOADED SQUARE CFST COLUMN TO RC BEAM JOINTS STIFFENED BY DIAGONAL RIBS

Dan Gan [1], Hua-Xuan Tang [1], Wen Li [1], Zheng Zhou [2, *], Xu-Hong Zhou [1] and Zhen-Ming Chen [3]

[1] *School of civil engineering, Chongqing University, Chongqing , China*

[2] *College of civil engineering, Hunan University, Changsha , China*

[3] *China Construction Steel Structure Engineering Corp., LTD, Shenzhen 518118, China*

* (*Corresponding author: E-mail:* zhouzhengchn@126.com)

ABSTRACT

This work proposes a partially through-beam joint system to connect square concrete-filled steel tubular (CFST) columns and reinforced concrete (RC) beams. In the system, the holes in the steel tube allow longitudinal beam reinforcements to be continuous through the joint zone to achieve direct load-transfer of the beam, and the square steel tube with holes is strengthened by welding diagonal ribs located at the corners of the steel tube. Finite element (FE) analyses on joints with RC beams were carried out based on verified models. The analysis results showed that diagonal ribs welded to the joint tube confined the concrete in the joint zone efficiently and made up for the reduction in axial load capacity caused by the holes of the steel tube, so the joint system can meet the requirements of strong-joint weak-component under axial compression with ease. Finally, mechanics-based models and axial strength equations of joints were proposed, and the predicted results agreed well with the FE results. These results proved that the square CFST column to RC beam joints stiffened by diagonal ribs were feasible and can be applied in engineering practice based on reasonable design .

1. Introduction

Concrete-filled steel tubular (CFST) columns get more and more applications as the main structural elements for resisting both vertical and lateral loads in multistory and high-rise buildings [1–4]. Compared with the circular CFST columns, the square CFST column has relatively large bending stiffness, high bending capacity and convenient construction, and has been well applied in engineering. Square CFST columns are usually connected to steel beams or reinforced concrete (RC) beams. In consideration of the cost, square CFST column to RC beam joints are widely used in China [5].

Various joint systems connecting CFST columns with RC beams have been proposed. Generally, there are two types of joint systems, namely through-column and through-beam joints, as shown in Fig. 1. In the through-column

joint (Fig. 1 (a)), the column steel tube is continuous through the joint zone, and the longitudinal reinforcements of RC beams are usually connected to steel corbels or stiffening rings which stiffen the joint zone and transfer both the shearing forces and bending moments [6,7]. In the through-beam joint (Fig. 1 (b)), the column steel tube is discontinuous, and the beam longitudinal reinforcements pass through the joint zone directly. Besides, the ring beam and column longitudinal reinforcements are used to strengthen the joint zone and to compensate for the reduction in axial load capacity caused by the discontinuous column tube [8–13]. Nevertheless, for through-column joints various stiffeners such as stiffening rings are needed to transfer the force from the reinforcements and welding on site cannot be avoided, and for through-beam joints the details for ring beams are complex and the protruded ring beams are architecturally undesirable.

(a) Through-column joint [7]

(b) Through-beam joint [10]

Fig. 1 Typical CFST column to RC beam joints

In recent years, a new kind of joint system, namely partially through-beam joints, was proposed due to the practical engineering demands, as shown in Fig. 2. In the partially through-beam joints, the holes in the hollow steel tube allowed beam longitudinal reinforcements to be continuous through the joint zone to transfer the bending moment and shearing force of the RC beam directly and effectively. Besides, the additional outer steel tube [14] or internal diaphragms [15] were welded to the joint steel tube to make up for the reduction in axial load capacity caused by the holes. The experimental and analytical results showed that these joint systems showed good axial and cyclic performance [14–16].

On the basis of previous research, a novel, more simplified and reliable partially through-beam joints was proposed in this work. As shown in Fig. 3,

diagonal ribs were welded to the edge of the hole to confine concrete in the joint zone and to co-carry the axial load. The square CFST columns stiffened by diagonal ribs were experimentally and analytically evaluated by the authors [17,18]. The results showed that: 1) the diagonal ribs changed the buckling mode and effectively delayed the local buckling of the square steel tube; 2) the diagonal ribs not only confined the steel tube and concrete, but also co-carried the axial load; 3) in comparison to square CFST columns with other stiffeners, the columns with diagonal ribs had higher strength, better ductility and larger energy dissipation capacity under the same steel ratio. Consequently, the newly proposed square CFST column to RC beam joints stiffened by diagonal ribs are anticipated to possess good mechanical properties.

(a) Joint with rectangular holes [14]

(b) Stiffened interior joint [15]

Fig. 2 Typical partially through-beam joints

However, it remains questionable that whether the proposed joint system can meet the requirements of the strong-joint weak-component under axial compression due to the holes in the joint steel tube. In this work, the feasibility of square CFST column to RC beam joints stiffened by diagonal ribs was carried out, and the axial compression behavior of the joints was studied through finite element (FE) analyses using ABAQUS. The FE models were verified by the test results in relevant literature, followed by extensive parametric analyses. Finally, based on the analytical results, the mechanics-based models and axial strength equations for the joints were proposed.
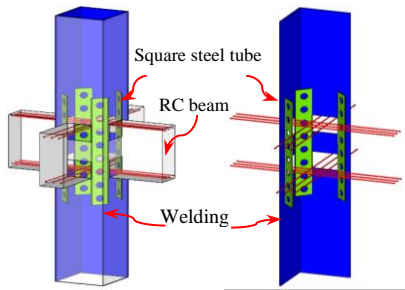

Fig. 3 Square thin-walled CFST column to RC beam joints

2.   Finite element model

2.1. Model description

(1) Benchmark model

Fig. 4 shows the details of the benchmark model. The width (B_c) and height (H_c) of the column were 300 mm and 1400 mm, respectively. The width (B_b) and height (H_b) of the beam were 150 mm and 300 mm, respectively. The width of the end sub-plate (b) was 75mm, namely the diagonal ribs were welded at 1/4 of the column width (i.e., $b=1/4B_c$). The thickness of the diagonal rib (t_s) and steel tube (t_t) were taken as 8mm. The spacing between two adjacent holes (s), the diameter of holes in the diagonal ribs (d) and the width of diagonal ribs (b_s) were 75mm, 25mm and 106.07mm, respectively. The ratio of hole area to the beam cross-sectional area was defined as the hole ratio of joint steel tube (ρ) (i.e., $\rho=2b_h/H_b$), which was 0.5 in the benchmark model. The concrete compressive strength (f_c) was 40MPa and the steel yield strength (f_y) was 345MPa. The yield strength of beam longitudinal reinforcements was 400MPa. The studied parameters are listed in Table 1.

(2) Modeling method

The concrete was modeled by solid element (type C3D8R). For concrete under compression, the Concrete Damaged Plasticity (CDP) model was used to model concrete, and the stress-strain relationships proposed by Han et al.[1] and GB50010 2010 [19] were applied for the column and beam concrete, respectively. For concrete under tension, the stress-strain model was obtained by defining the tensile stress and tensile fracture energy presented in CEB-FIP MC90 [20]. The elastic modulus and Poisson's ratio of concrete were 4730*sqrt(f_c) and 0.2 [21], respectively.

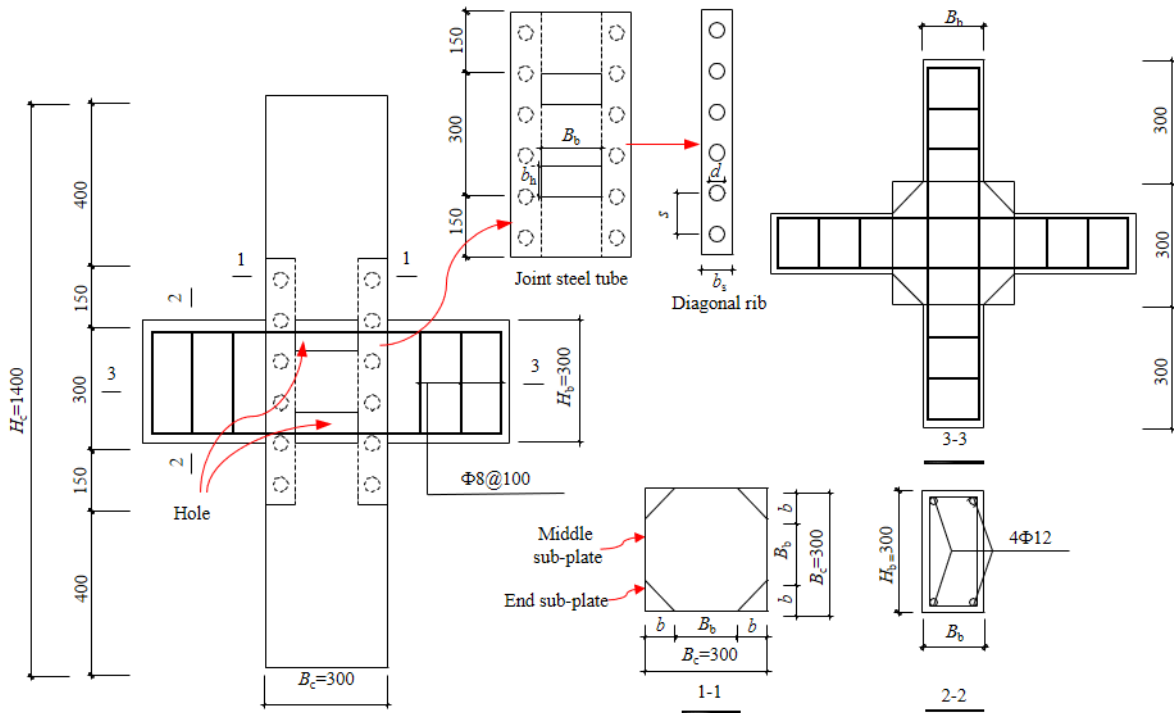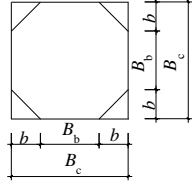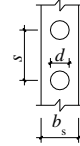**Fig. 4** Details of the benchmark model (units: mm)

Table 1
Joint parameters

Parameter	Variables	Fixed values
Width of end sub-plate (b)	$0.25B_c$, $0.27B_c$, $0.28B_c$, $0.30B_c$, $0.32B_c$, $0.33B_c$	$1/4B_c$
Width-to-thickness ratio of steel tube (B_c/t_t)	18.75, 21.43, 25, 30, 37.5, 50	37.5
Ratio of diagonal rib thickness to tube thickness (t_s/t_t)	0, 0.25, 0.50, 0.75, 1.00, 1.25, 1.50	1.00
Diameter of hole in diagonal rib (d)	$0b_s$, $0.20b_s$, $0.24b_s$, $0.40b_s$, $0.60b_s$, $0.70b_s$	$0.24b_s$
Spacing between two adjacent holes (s)	$3d$, $4d$, $5d$, $6d$, $9d$	$3d$
Hole ratio of joint steel tube (ρ)	0.5, 0.6, 0.7, 0.8, 0.9, 1.0	0.5
Concrete compressive strength (f_c: MPa)	30, 40, 50, 60, 70, 80	40
Steel yield strength (f_y: MPa)	235, 345, 460, 550, 600, 700, 800	345

Steel tubes and diagonal ribs were simulated by shell element (type S4R), and reinforcements were simulated by truss element (type T3D2). The elastic-perfectly plastic stress-strain model was adopted for steel. The elastic modulus and Poisson's ratio of steel were selected as 206GPa and 0.3, respectively.

In the FE model, diagonal ribs and beam reinforcements were embedded in the concrete. The interface between the steel tube and concrete was modeled by surface-to-surface contact interaction, where the hard contact was used for the normal behavior and Mohr-Coulomb friction model with a fiction coefficient of 0.6 was used for the tangential behavior. The column end was fixed, and only the vertical degree of freedom of the column top was released.

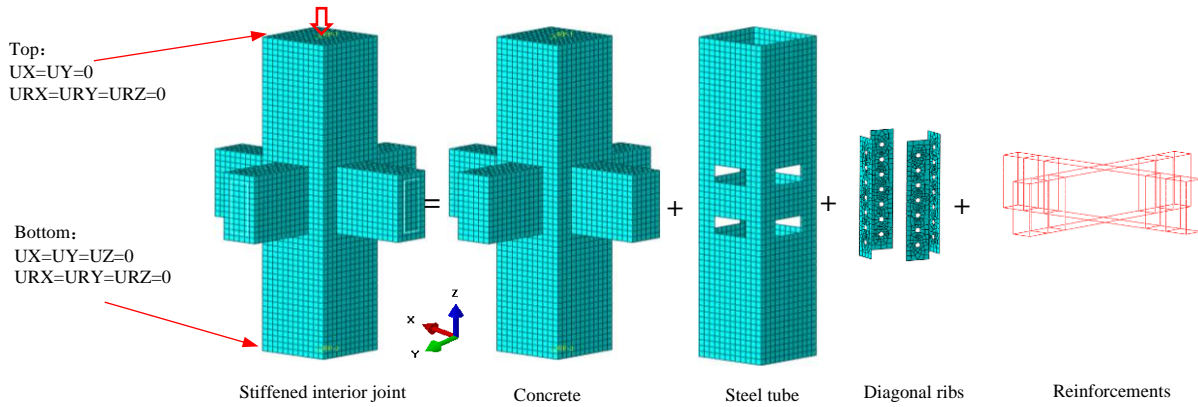As shown in Fig. 5, the mesh size was 1/10 of the column width based on sensitivity study.

Top:
UX=UY=0
URX=URY=URZ=0

Bottom:
UX=UY=UZ=0
URX=URY=URZ=0

Stiffened interior joint   Concrete   Steel tube   Diagonal ribs   Reinforcements

Fig. 5 FE model of joints

2.2. Model verification

(1) Square CFST column stiffened by diagonal ribs

Typical square CFST columns stiffened by diagonal ribs in previous tests [18] were simulated. As shown in Fig. 6, the FE model well predicted the initial stiffness and peak strength.

(2) TRC column to RC beam joints

Similar joint specimens in the literature [11,12] were simulated. As shown in Fig. 7 and Fig. 8, the failure modes, initial stiffness and peak strength were in good agreement with test results. Based on these verifications, the proposed model can be used for further analyses.
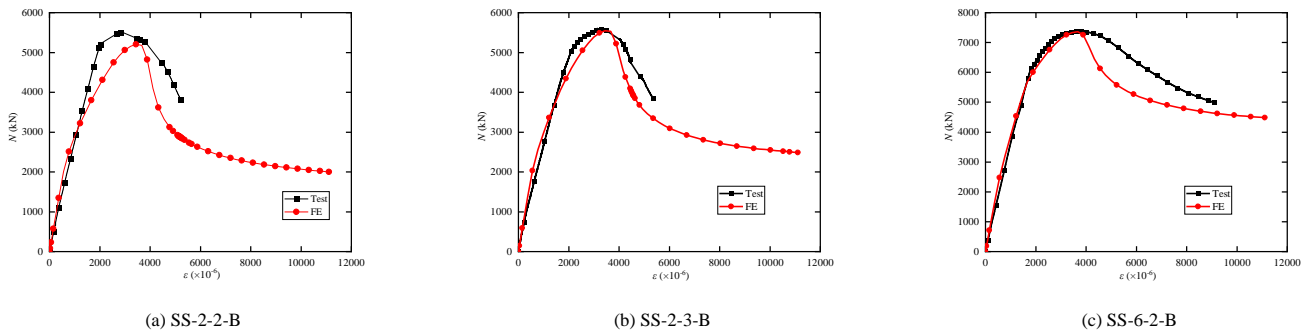

(a) SS-2-2-B

(b) SS-2-3-B

(c) SS-6-2-B

Fig. 6 Comparison on FE and experimental results for square CFST columns stiffened by diagonal ribs

(a) B-240-120-2

(b) B-240-120-3

(c) B-240-120-4
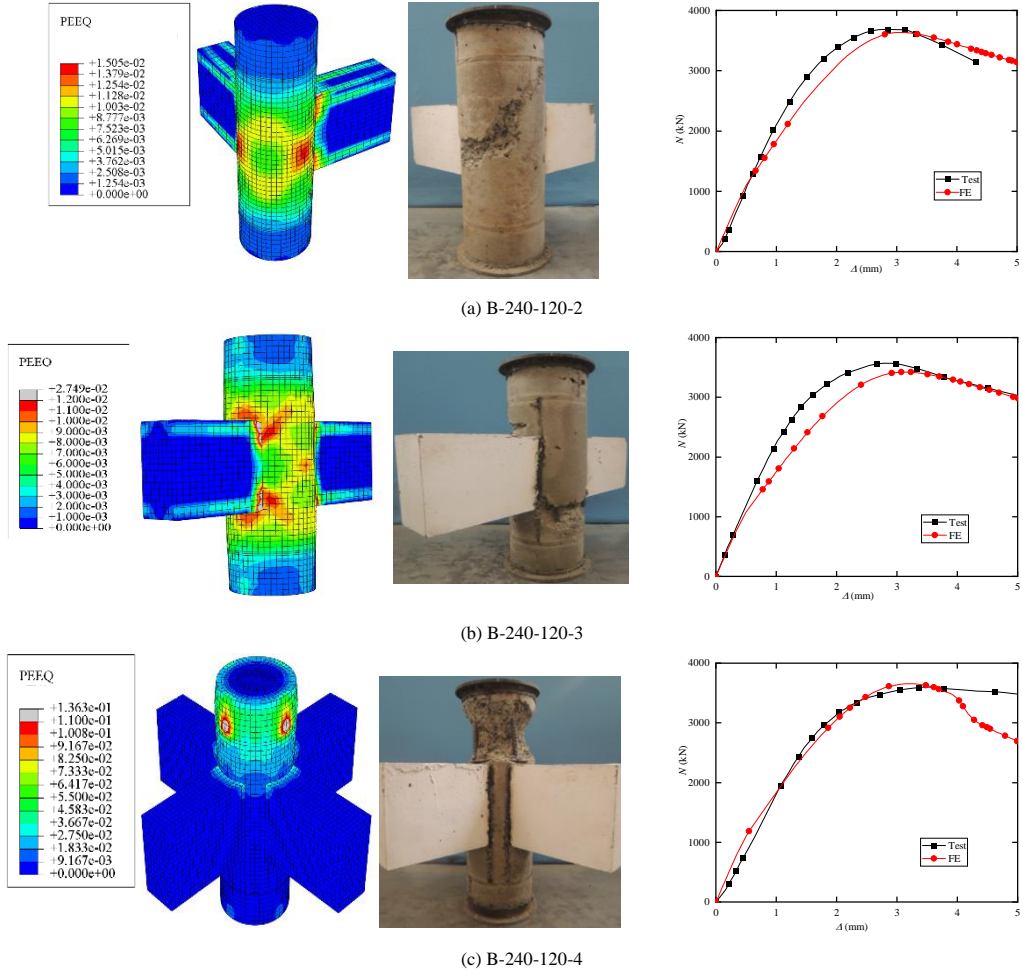
Fig. 7 Comparison on FE and experimental results for circular TRC column to RC beam joints

(a) SC(GS)-140-2-S
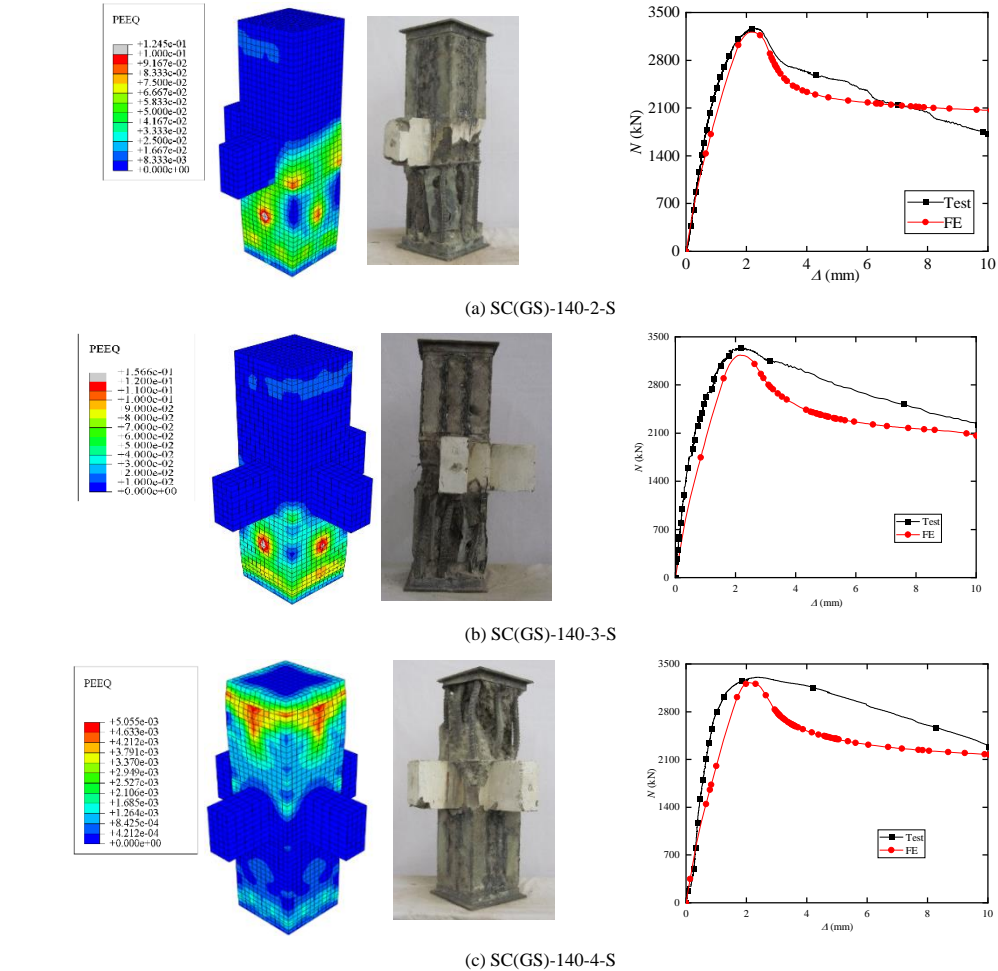

(b) SC(GS)-140-3-S

(c) SC(GS)-140-4-S

Fig. 8 Comparison on FE and experimental results for square TRC column to RC beam joints

3. Parametric study

As shown in Fig. 9, two failure modes for the interior joints stiffened by diagonal ribs were observed based on the strain distribution of the concrete, namely the joint failure and column failure.

(1) Effect of end sub-plate width (b) and hole ratio of joint steel tube (ρ)

Fig. 10(a) shows the effect of b. The failure mode and peak strength remained almost unchanged with b increased from $1/4B_c$ to $1/3B_c$, and the requirements of the strong-joint weak-component under axial compression were satisfied. Consequently, the end sub-plate width was suggested to be $1/4 B_c$ - $1/3B_c$ (i.e., $b = 1/4B_c$ -$1/3B_c$). Note that the beam width also changed with variation of b, since the diagonal ribs were welded to the edge of the hole.

As shown in Fig. 10(b), the peak strength was unchanged due to the same column failure with ρ smaller than 0.9. However, the strength was reduced obviously and the failure mode was changed to joint failure due to larger ρ of 1.0. Therefore, ρ should be no larger than 0.9 to avoid excessively weakening the joint steel tube and to achieve the strong-joint weak-component. Additionally, the potential direct shear failure of the interface between the column and beam would occur when ρ was smaller than 0.5 [22]. Consequently, it is recommended the hole ratio lager than 0.5 while smaller than 0.9 (i.e., ρ = 0.5-0.9).
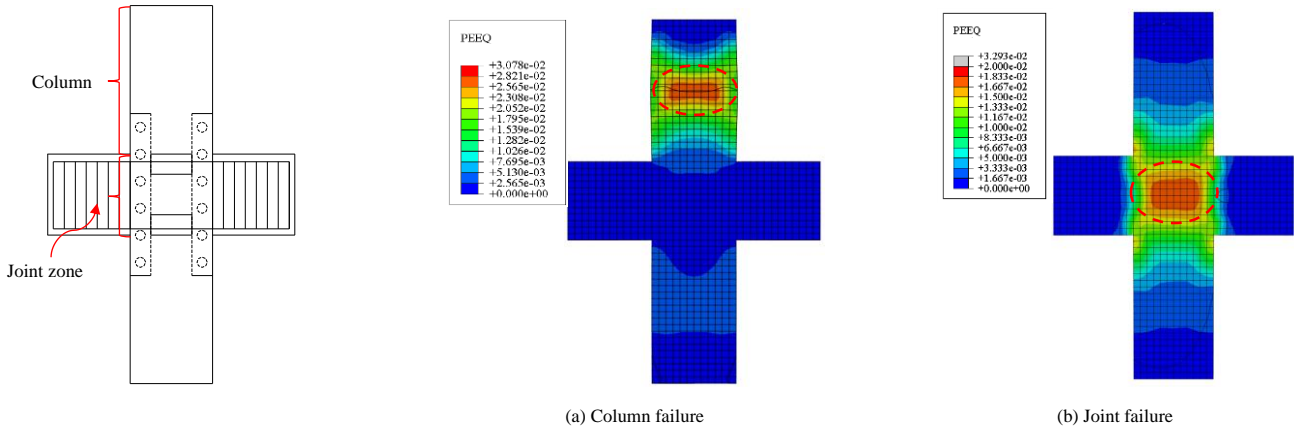

(a) Column failure

(b) Joint failure

Fig. 9 Failure modes of joints stiffened by diagonal ribs

(2) Effect of thickness of joint steel tube (t_t) and thickness of diagonal rib (t_s)

As shown in Fig. 11(a), the peak strength was increased with larger t_t, whereas the failure mode remained unchanged, as the load capacity provided by the column and joint zone varied simultaneously.

As shown in Fig. 11(b), thicker t_s increased the load capacity of the joint zone, and thus the peak strength was enhanced significantly for specimens with joint failure. However, the strength enhancement was slight after the value of t_s/t_t larger than 0.75, as the failure mode was changed to the column failure and the load capacity was provided by the unstiffened CFST column. For ease of design, the thickness of the diagonal rib was suggested to be the same as that of the steel tube (i.e., t_s/t_t =1.0).

(3) Effect of concrete strength (f_c) and steel yield strength (f_y)

As showed in Fig. 12, the strength increased linearly with larger f_c and f_y, as f_c and f_y didn't change difference of the confinement stress between different zones, and thus the failure mode was unchanged.

(4) Effect of spacing between two adjacent holes (s) and diameter of holes (d)

As shown in Fig. 13(a), the spacing of holes affected the strength little and the failure mode was unchanged. This was attributed to fact that the effective cross-sectional areas of diagonal ribs were unchanged. According to Zhou et al. [23], the spacing was recommended at least 2.25 times the hole diameter (i.e., $s \geq 2.25d$) to avoid the potential highly stressed regions between two adjacent concrete dowels.

Fig. 13(b) showed that the strength of specimens decreased with d increased from 0 to $0.7b_s$, but the strength reduction was within 3%, and the failure mode was also unchanged. A larger d could facilitate concreting, increase the anchorage and improve the load transfer between the steel and concrete, while also weak the diagonal ribs. Therefore, the hole diameter (d) is recommended to be with the range of $0.2-0.7b_s$ (i.e., $d = 0.2-0.7b_s$).
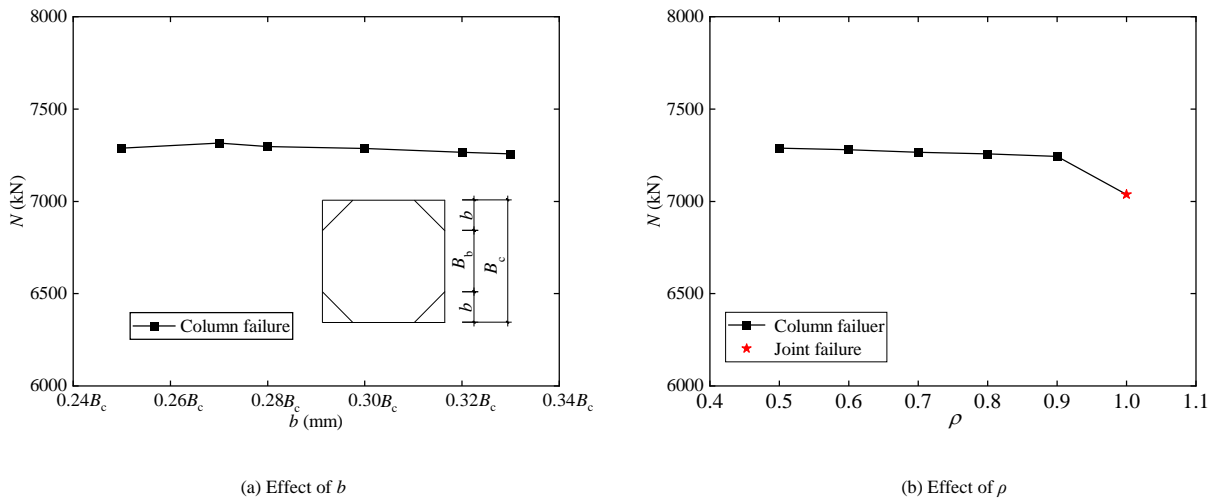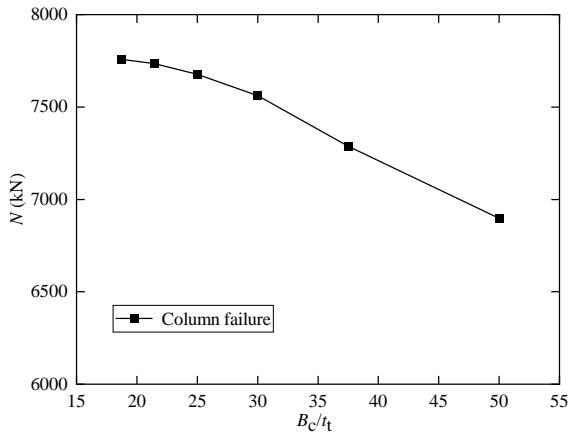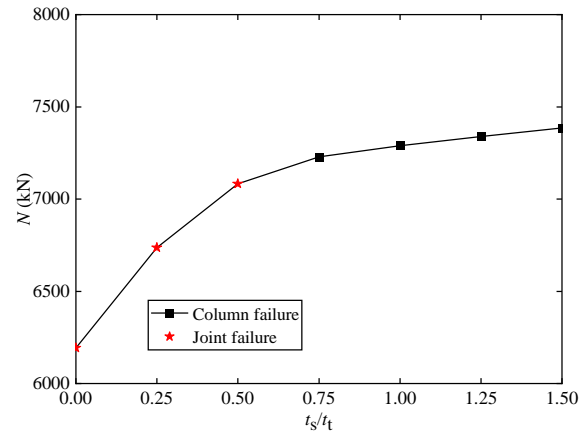

(a) Effect of b

(b) Effect of ρ
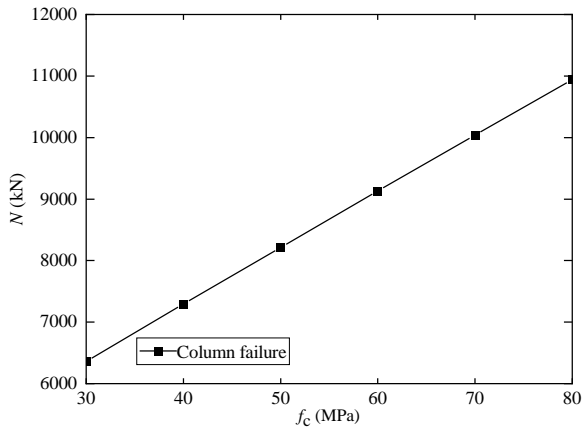
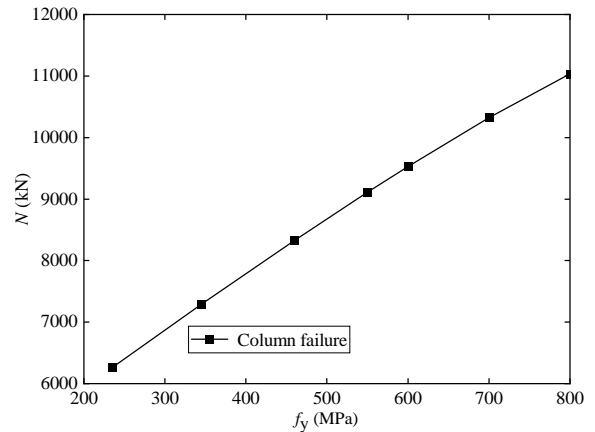**Fig. 10** Effect of b and hole ratio of joint steel tube

(a) Effect of *b/t*t

(b) Effect of *t*s/*t*t

Fig. 11 Effect of *t*s and *t*t
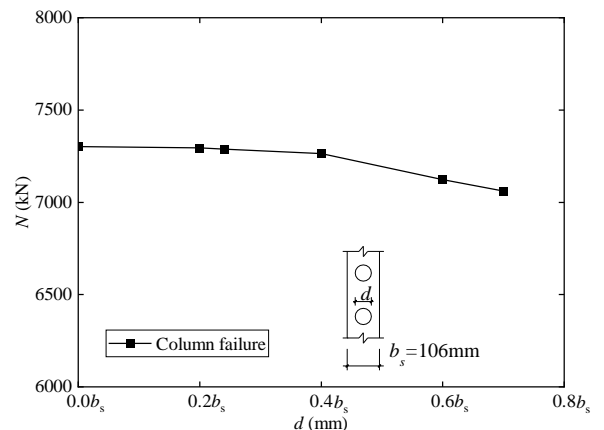

(a) Effect of *f*c

(b) Effect of *f*y

Fig. 12 Effect of *f*c and *f*y
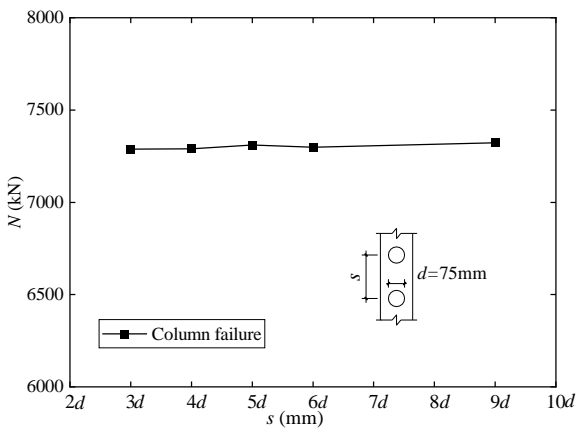
(a) Effect of *s*

(b) Effect of *d*

Fig. 13 Effect of *s* and *d*

4. Prediction for axial load capacity of joint zone

4.1. Plastic stress distribution method

In this section, the plastic stress distribution (PSD) method was firstly used to predict the axial load capacity of the joint zone, as the PSD method was widely used as the primary method for calculating the strength of steel-concrete composite members [24,25]. In the PSD method, steel components are assumed to have attained their yield stress in either tension or compression and the concrete is assumed to have attained their compressive stress in compression [24]. Tension strength of the concrete is neglected. Note that neglecting the local buckling of the steel tube was reasonable, as the column steel tubes were designed to meet the width-to-thickness ratio limitations in typical standards [26].

The axial load capacity of the joint zone depended on the minimum load capacity provided by Zones I and II, as shown in Fig. , and thus the load capacity of Zone I was focused on due to the holes. Consequently, the axial load capacity of joint zone (N_j) was calculated as

$$N_j = A_c f_c + A_{tj} f_{ty} + A_{sj} f_{sy} \tag{1}$$

Where A_c, A_{tj} and A_{sj} are the net cross-sectional areas of the concrete, joint steel tube and diagonal rib, respectively. f_c, f_{ty} and f_{sy} are the concrete compressive strength, and yield strength of the steel tube and diagonal rib, respectively.
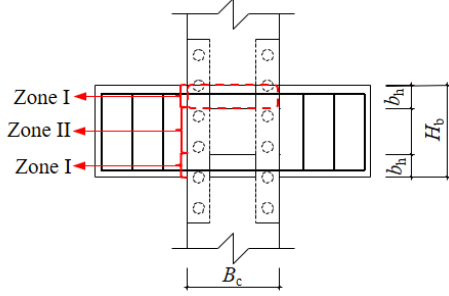

Fig. 14 Diagram of joint zone

As shown in Fig. 15, the average ratio and standard deviation of the calculated to the FE predicted were 0.827 and 0.045, respectively, indicating that the PSD method was very conservative .
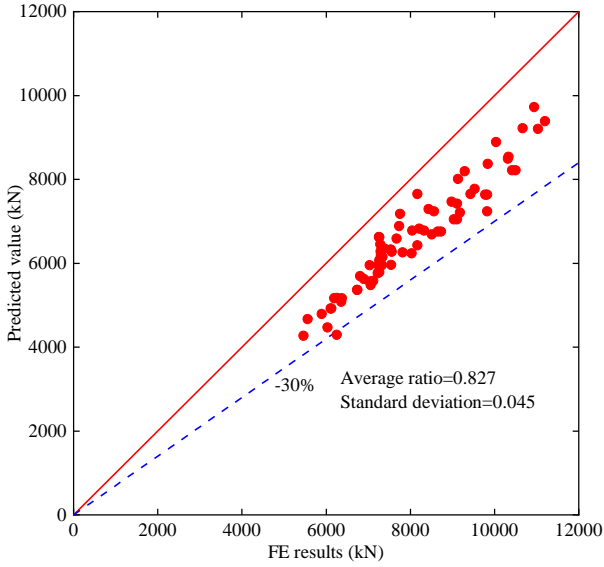

Fig. 15 Comparison between FE results and computation results from PSD method

4.2. Proposed model

Based on the above-mentioned calculation results, the PSD method was too conservative due to the unconsidered confinement from the steel tube and diagonal ribs to the concrete. Therefore, in this section, the axial load capacity for the joint zone was calculated based on the confined concrete theory [27]. It was assumed that the arching action acted in the form of second-degree parabolas with an initial tangent angle of 45° both in the horizontal and vertical directions. Both diagonal ribs and steel tubes were considered to not only confine the concrete through horizontal tensile stress, but also carry vertical forces through longitudinal compressive stress.

The axial load capacity of the joint zone (N_j) was calculated as:

$$N_j = A_c \sigma_{cc} + A_{tj} \sigma_{tv} + A_{sj} \sigma_{sv} + N_{jb} \tag{2}$$

$$\sigma_{cc} = \begin{cases} f_c'\left(-1.254 + 2.254\sqrt{1 + 7.94\dfrac{f_r'}{f_c'}} - 2\dfrac{f_r'}{f_c'}\right), & f_c' \leq 50\text{MPa}^{[24]} \\ f_c'\left(-0.413 + 1.413\sqrt{1 + 11.4\dfrac{f_r'}{f_c'}} - 2\dfrac{f_r'}{f_c'}\right), & f_c' \geq 50\text{MPa}^{[25]} \end{cases} \tag{3}$$

$$f_r' = k_e f_r \tag{4}$$

Where σ_{cc} is the compressive strength of confined concrete. σ_{cc}, σ_{tv} and σ_{sv} are the compressive strength of confined concrete and the vertical compressive stress of the steel tube and diagonal rib, respectively. N_{jb} is the load capacity provided by the RC beam. f_r' and f_r are the effective confinement stress and confinement stress, respectively. k_e is the confinement effectiveness coefficient.

For Zone I, the confinement stress was provided by the joint steel tube with holes and diagonal ribs. The effectively confined zones were shown in Fig. 16. Note that the beam longitudinal reinforcements were mainly used to resist the bending moment and thus their confining effect was ignored. Therefore, the effective confinement stress was calculated by

$$f_r' = k_{ev} k_{eh} f_r \tag{5}$$

Where k_{ev} is the vertical confinement effectiveness coefficient of Zone I. k_{eh} is the horizontal confinement effectiveness coefficient for the square steel tube with diagonal ribs.
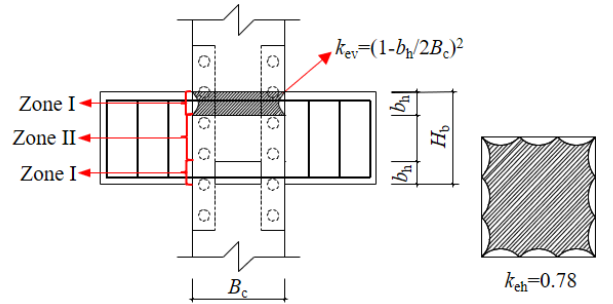

Fig. 16 Effectively confined zones

The confinement stress f_r from the diagonal ribs stiffened square steel tube with holes was calculated by:

$$2\sigma_{th} t_t (1 - \rho) + 2\sigma_{sh}\cos 45° t_s (1 - \frac{d}{s}) = f_r (B_c - 2t_t) \tag{6}$$

Where σ_{th} and σ_{sh} are horizontal tensile stress of the steel tube and diagonal rib. d and s are the diameter and spacing of the holes on one diagonal rib, respectively. ρ is the hole ratio.

According to Sakino et al. [28], the vertical compressive stress (σ_{tv}) and horizontal tensile stress (σ_{th}) of the steel tube were taken as $0.89f_{yt}$ and $0.19f_{yt}$, respectively, which satisfied the von Mises criteria since the steel tube yielded at the peak load. Analogously, the vertical compressive stress of diagonal ribs σ_{sv} and σ_{sh} were respectively taken as $0.89f_{ys}$ and $0.19f_{ys}$ due to no local buckling.

The load capacity provided by the RC beams was [16]

$$N_{jb} = \beta f_c' \alpha n b_h B_b \tag{7}$$

Where β is the uneven distribution coefficient of the concrete compressive stress of the diffusion cross-section and is taken as 0.33. α is the diffusion angle of local compression and is taken as 0.5. n is the number of orthogonal beams. B_b and b_h is the beam width and hole height.

As shown in Fig. 17, the average ratio and standard deviation of the calculated to the tested and FE predicted is 0.988 and 0.064, respectively. Therefore, the proposed axial load capacity equations well predicted the strength of the joint zone stiffened by diagonal ribs.
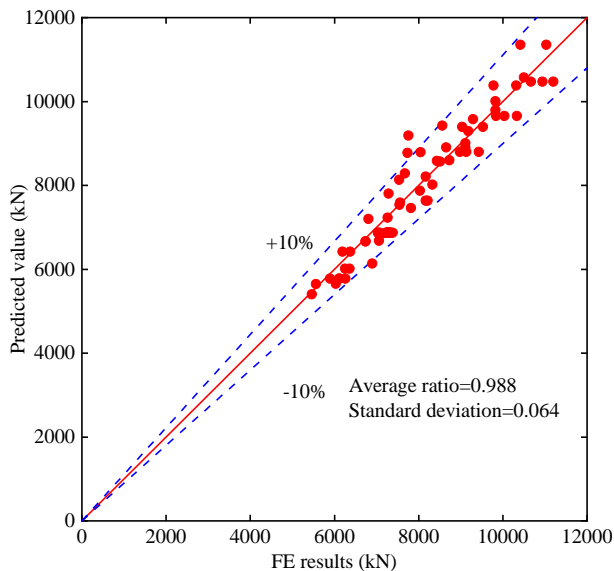
Fig. 17 Comparison between FE results and predicted results from proposed model

5. Conclusions

In this work, the feasibility of square CFST column to RC beam joints

stiffened by diagonal ribs was carried out, and the axial compression behavior of the joints was studied through FE analyses. The following conclusions can be drawn:

(1) Two failure modes, namely joint failure and column failure, were observed based on parametric analyses. The results showed that the increase of material strength enhanced the joint strength linearly, while not affected the failure mode; the thickness of the diagonal rib and hole ratio affected both the joint strength and the failure mode.

(2) The strong-joint weak-componen can be achieved without conducting calculation once the following joint details were satisfied, namely the diagonal rib was welded at 1/4 to 1/3 times the column width (i.e., $b = 1/4B_c$-$1/3B_c$), the hole ratio was larger than 0.5 while smaller than 0.9 (i.e., the hole area to the beam cross-sectional area ratio $\rho = 0.5$-0.9), the thickness of the diagonal rib was the same as that of the steel tube, the spacing between two adjacent holes was no less than 2.25 times of the hole diameter (i.e., $s \geq 2.25d$), and the hole diameter was within 0.2-0.7 times the diagonal ribs width (i.e., $d = 0.2$-$0.7b_s$).

(3) The plastic stress distribution (PSD) method was found to be very conservative with the average ratio and standard deviation of 0.827 and 0.045, respectively, as the confinement from the steel tube and diagonal ribs to the concrete was ignored. Based on the confined concrete theory, the mechanics-based models were proposed and agreed well with the FE results with the average ratio and standard deviation of 0.98 and 0.064, respectively.

Acknowledgements

References

[1] Han L.H., Li W, Bjorhovde R., "Developments and advanced applications of concrete-filled steel tubular (CFST) structures: Members", Journal of Constructional Steel Research. 100, 211–228, 2014.
[2] Kang X.J., Liu Y.H., Zhao L., Yu Z.X., Zhao S.C. and Tang H., "Dynamic response analysis method for the peak value stage of concrete-filled steel tube beams under lateral impact", Advanced Steel Construction. 15, 329–337,2019.
[3] Liu S.W., Liu Y.P., Chan S.L., "Advanced analysis of hybrid steel and concrete frames: Part 1: Cross-section analysis technique and second-order analysis", Journal of Constructional Steel Research. 70, 326–336, 2012.
[4] Liu S.W., Liu Y.P., Chan S.L., "Advanced analysis of hybrid steel and concrete frames: Part 2: Refined plastic hinge and advanced analysis", Journal of Constructional Steel Research. 70, 337–349, 2012.
[5] Wang D.S. and Zhou J.L., "Development and prospect of hybrid high-rise building structures in China", Journal of Building Structures (in Chinese). 31, 62–70, 2010.
[6] Yu H. and Zha X.X., "Seismic behavior of CFST column to beam joint without welding in construction field: experiment and FE analysis", Industrial Construction (in Chinese). 41, 15–19, 2011.
[7] Nie J.G., Wang Y.H., Tao M.X., "Research and optimization on laminated steel tube column-concrete beam joints with outer stiffening ring", Sci. China Technol. Sci. 56, 1282–1293, 2013.
[8] Nie J.G., Bai Y., Cai C.S., "New Connection System for Confined Concrete Columns and Beams. I: Experimental Study", Journal of Structural Engineering. 134, 1787–1799, 2008.
[9] Tang X.L., Cai J., Chen Q.J., Liu X.P. and He A., "Seismic behaviour of through-beam connection between square CFST columns and RC beams", Journal of Constructional Steel Research. 122, 151–166, 2016.
[10] Chen Q.J, Cai J., Bradford M.A., Liu P.X. and Wu Y., "Axial Compressive Behavior of Through-Beam Connections between Concrete-Filled Steel Tubular Columns and Reinforced Concrete Beams", Journal of Structural Engineering. 141, 04015016, 2015.
[11] Zhou X.H., Li B.Y., Gan D., Liu J.P.and Chen Y.Frank., "Connections between RC beam and square tubed-RC column under axial compression: Experiments", Steel and Composite Structures. 23, 453–464, 2017.
[12] Zhou X.H., Cheng G.Z., Liu J.P., Gan D. and Chen Y.Frank, "Behavior of circular tubed-RC column to RC beam connections under axial compression", Journal of Constructional Steel Research. 130, 96–108 ,2017.
[13] Chen. F., Li G.C., Zhang L. and Yang Z.J., "Experimental and numerical investigation on seismic performance of ring-beam connection to gangue concrete filled steel tubular columns", Advanced Steel Construction. 18, 506–516, 2022.
[14] Yuan H.X., Wu Z.K., Du X.X., Guo J.C., Wen S.Q. and Wen Y.J., "Experimental study on structural performance of joint between RC beam with continuous reinforced bars and CFST column with rectangular openings", Engineering Journal of Wuhan University (in Chinese). 55, 356–365, 2022.
[15] Gan D., Zhou Z., Zhou X.H. and Tan K.H., "Seismic Behavior Tests of Square Reinforced Concrete–Filled Steel Tube Columns Connected to RC Beam Joints", Journal of Structural Engineering. 145, 04018267,2019.
[16] Gan D., Zhao Z.X., Zhou Z. and Zhou X.H, "Axial compression behavior of reinforced concrete beam to square thin-walled concrete-filled steel tube column joints stiffened by internal diaphragms", Structural Concrete. 18, 2022.
[17] Zhou Z., Gan D., Zhou X.H, "Cyclic-shear behavior of square thin-walled concrete-filled steel tubular columns with diagonal ribs", Engineering Structures. 259, 114177, 2022.
[18] Zhou Z., Gan D., Zhou X.H., "Improved Composite Effect of Square Concrete-Filled Steel Tubes with Diagonal Binding Ribs", Journal of Structural Engineering. 145, 04019112,2019.
[19] GB 50010-2010: Code for design of concrete structures 2010., Minstry of Housing and Urban-Rural Development of the People's Republic of China, Beijing, China, 2016.
[20] CEB: CEB-FIP Model Code 1990., Thomas Telford Services Lt, Lausanne, Switzerland, 1993.
[21] ACI 318M-08: Building Code Requirements for Structural Concrete, American Concrete Institute, Detriot(Michigan), America, 2019.
[22] Gan D., Zhou Z., Yan F. and Zhou X.H., "Shear Transfer Capacity of Composite Sections in Steel Tubed-Reinforced-Concrete Frames", Structures. 12, 54–63, 2017.
[23] Zhou X.H., Zhou Z., Gan D., "Analysis and design of axially loaded square CFST columns with diagonal ribs", Journal of Constructional Steel Research. 167, 105848, 2020.
[24] Eurocode 4: Design of composite steel and concrete structures. Part 1.1: General rules and rules for building.European Committee for Standardization, Brussels: CEN, 2004.
[25] Specification for structural steel buildings, American Institute of Steel Construction, Chicago, USA, 2016.
[26] Yang C., Yu Z.X., Sun Y.P., Zhao L. and Zhao H., "Axial residual capacity of circular concrete-filled steel tube stub columns considering local buckling", Advanced Steel Construction. 14, 18, 2017.
[27] Mander J.B., Priestley M.J.N., Park R., "Theoretical Stress-Strain Model for Confined Concrete", Journal of Structural Engineering. 114, 1804–1826,1988.
[28] Sakino K., Nakahara H., Morino S. and Nishiyama I., "Behavior of Centrally Loaded Concrete-Filled Steel-Tube Short Columns", Journal of Structural Engineering. 130, 180–188, 2004.